University of North Carolina Asheville
Journal of Undergraduate Research
Asheville, North Carolina
Fall 2025

# Improving Processability of PTQ-10 Derivatives in Green Solvents through Hansen Solubility Parameters

Adam Wold

Department of Chemistry and Biochemistry
The University of North Carolina Asheville
One University Heights
Asheville, North Carolina 28804 USA

Faculty Mentor: Dr. Jeromy Rech

## Abstract

Harvesting solar energy can be a meaningful path towards a stable and renewable energy future. Outside of traditional silicon solar panels, an emerging technology of organic solar cells (OSC) shows promise. Along with rapidly improving efficiencies over 20%, OSCs offer unique benefits of flexibility, low cost, and semitransparency; however, the processing of OSC materials is problematic due to the use of costly and toxicity solvents. The purpose of this work is to develop green solvent processable polymers through two different approaches. First, through a combination of computational and experimental means, we aim to find new green solvents for current high-performance polymers, such as PTQ-10. Second, we aim to design novel solubilizing side chains for new conjugated polymers. This work applies Hansen Solubility Parameters (HSPs) to model the solubility of polymers in a variety of potential solvents. HSP are values derived from the intermolecular forces present in organic molecules and polymers. By determining the HSP values of a polymer, ideal solvents can be identified without rigorous guess-and-check methodology. From a synthetic standpoint, to avoid issues found in past oligo(ethylene glycol) side chain modification, we decided to work on adding side chains with a long alkyl segment capped with either an ionic or polar head. With HSP we can calculate the change in solubility with this new side chain and test green solvents with the new polymer. This work computationally finds three new solvents to dissolve PTQ-10 and determines synthetic procedure to add new side chains to PTQ-10's core.

## Introduction

The conscious effort towards renewable energy has been a topic of public debate for decades. This effort began with the acknowledgement of the unsustainable use of fossil fuels for

powering our daily lives. Since this revelation, various renewable energy sources have been explored, like hydropower, geothermal, wind, and solar. Despite these various renewable energy source options, fossil fuels still provide 83% of the energy the world uses.[1] This rate of consumption is not only unsustainable but predicted to exhaust fossil fuel deposits by 2060.[2]

Of the previously mentioned renewable energy options, solar has been one of the most popular due to its widespread application and limited maintenance.[3] The current solar energy market is dominated by monocrystalline silicon solar panels, which can achieve  One of the reasons efficiency over 25%.[4] These cells work through two different layers of doped crystalline silicon, one being a p-type (often boron-doped) and the other being an n-type (often phosphorus doped) as seen in **Figure 1**. When light hits the material, excited electrons (and corresponding holes) move towards an external electric field. This movement of electrons creates a current that can be used to power electronic devices, same as any other type of electricity.[5]

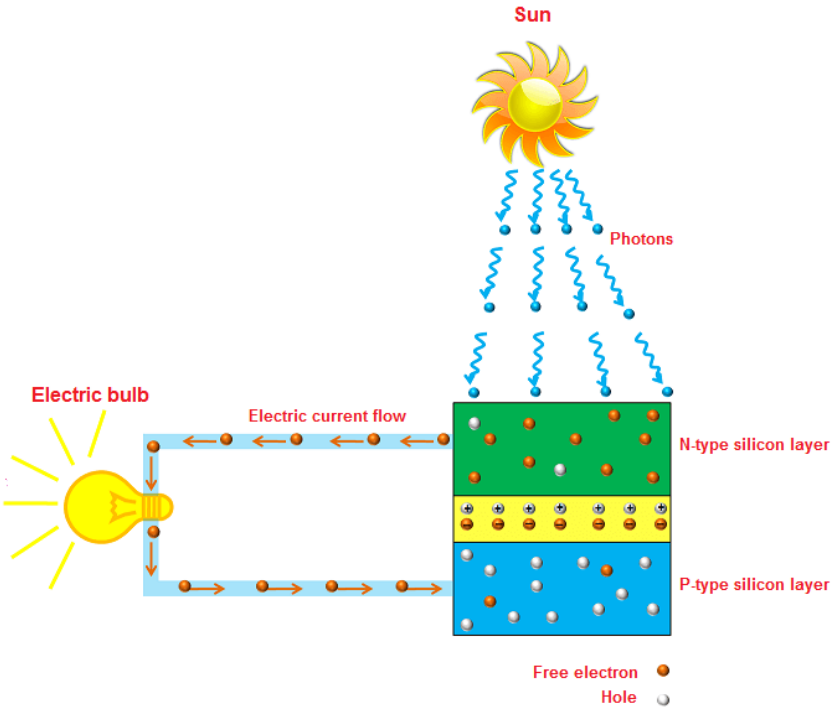


**Figure 1**. A visual representation of how silicon solar panels work.[6]

Recently however, attention has shifted towards emerging solar energy options, like dye-sensitized, perovskites, and polymer-based photovoltaics, the latter of which is also often referred to as organic solar cells (OSC's). OSC interest has improved drastically due to their recent development in cell efficiencies, rising from 12% efficiency in 2017 to over 20% cell efficiency today.[7-9] OSCs are made of conjugated polymers that are synthesized to generate charge upon photoexcitation. In these cells, donor (often polymer) and acceptor (often small molecule) compounds are paired to form excitons. Excitons are a concentration of energy created by an excited electron and corresponding hole. These donor and acceptor compounds carry the exciton and hole towards an interface where that exciton is split into independent electrons and holes, consistent with other solar technology. This use of excitons and conjugated polymers is unique to OSCs and not used in traditional solar cells. These conjugated polymers, or plastics, have been developed for decades as their low-cost production, flexibility, semi-transparency, and light weight makes them

highly sought after.[10-13] These properties make them ideal for applications like portable solar chargers or solar panels implemented in clothing. Previous research even illustrates the ability of these OSCs to work over greenhouses without harming the plants underneath due to the difference in light absorption between OSCs and plants.[14,15]

Organic solar cells have been proven relevant in academia; however, this success has not translated to commercial success for several reasons. The first reason is that larger conjugated polymers with higher efficiencies have high synthetic complexities as well. An example of this is D18-Cl, one of the highest efficiency conjugated polymers made to date. The chemical structure of D18-Cl is shown in **Figure 2B**. D18-Cl has a synthetic route of twenty-eight steps, and many of these steps either go overnight.[7] The second reason is the instability of the conjugated polymers when exposed to many environmental conditions. Many of these organic materials can quickly degrade in the presence of water and air.[16,17] The third reason is that these plastics also require hazardous solvents like chloroform or dichlorobenzene to dissolve them, and these are not ideal for an industrial setting.[18] With plastic solar panels drastically increasing in efficiency over the last decade, it is more apparent than ever that the issues of synthetic complexity and hazardous solvents need to be addressed soon to allow commercial use.[19]

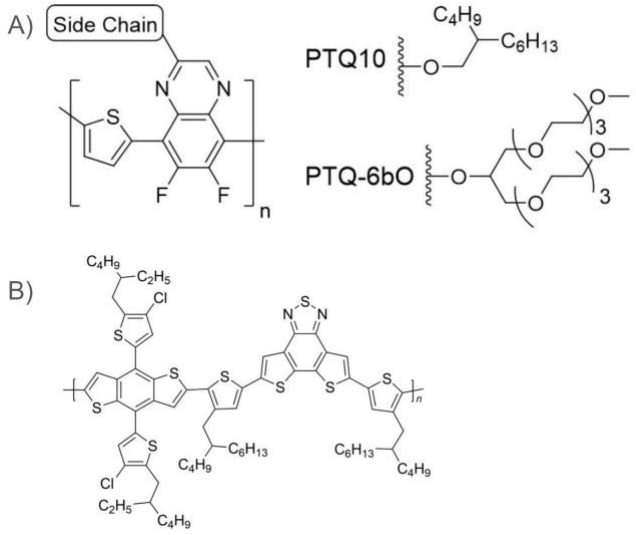


**Figure 2**. A) Chemical structure of PTQ-10, along with a derivative that has a new side chain to increase solubility. B) Chemical structure of a D18-Cl.

To make OSCs commercially available, these issues need to be addressed. We start this process by attempting to shift PTQ-10 towards green solvents. PTQ-10, shown in **Figure 2A**, is an organic solar cell donor polymer that maintains a low synthetic complexity. Impressively, this low synthetic complexity does not hinder its efficiency, with many reports over 18%.[20,21] This makes PTQ-10 ideal since we avoid synthetically complex molecules (like D18-Cl), and modifications to its structure are simple, making it easy to modify for solubility. Additionally, the You group recently published the derivative called PTQ-6bO, shown in **Figure 2A**, which use oligo(ethylene glycol) or OEG side chain.[19] While this modification of the side chain drastically improved the solubility in many greener solvents, there was a sharp decrease in the efficiency of the solar cell. In another work with OEG side chains, they saw their polymers drop in efficiency to a measly 2.15%.[26,27] This decrease in efficiency was likely caused by the increase of oxygen in their side chain. These oxygens were found to have caused a detrimental change in the polymers energy levels and morphology which disrupted

the absorption, charge separation, and charge transportation processes. Ultimately, these results show promise if we can find modifications which do not impact the core conjugated backbone.

Modifications of PTQ-10 are easily accessible in the synthetic route. **Figure 3** outlines the complete synthetic route for PTQ-10. This synthesis is made up of 5 steps, and the majority of them boast a yield over 80%. The fourth reaction in this sequence is the only one that requires modification to change the side chain, and thus solubility, which illustrates the ease of this modification.

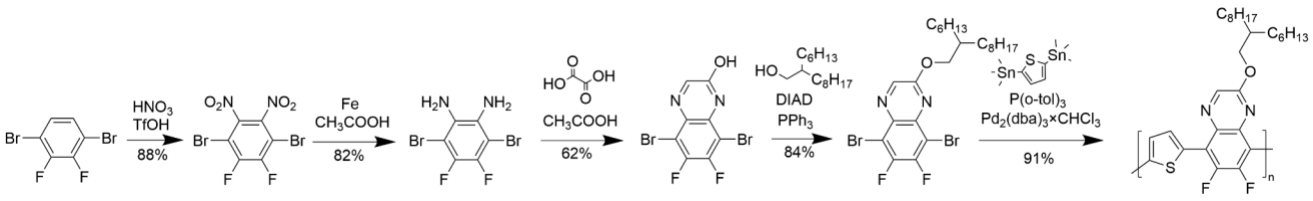


**Figure 3**. This is a common synthetic route to create PTQ-10.[22]

While most scientists agree that green solvents offer more safety and are environmentally friendly, the use of the word "green" is often done without ample evidence. Most commonly, this distinction is made for solvent which do not certain specific hazardous functional groups, like halogens and aromatic rings. This pattern recognition does not necessarily illustrate all the details of a solvent, however. This is why we obtain a comprehensive view of solvent "greenness" from GlaxoSmithKline's (GSK's) methods. GSK has provided a method to rank solvents from 1-10 based on how safe or green they are, inspired by their use in the pharmaceutical industry. Most of these considerations also lend well to the OSC processing, as they are based on categories like difficulty of disposal, environmental hazards, health hazards, and safety.[18] Common features in highly rated green solvents are simple, low boiling point alcohols, like ethanol.

In previous literature, PTQ-10's solubility has been measured using Hansen Solubility Parameters (HSP).[19] HSP are a mathematical way to value the strength of intermolecular forces in molecules, and with this mathematical representation we can understand the solubility of a polymer created in a given solvent. The HSP uses the premise of "like dissolves in like", so the closer values are between a solvent and a solute, the more likely they are to be soluble.[23] To find these values experimentally, an amount of the compound is mixed in a solvent at a set temperature. This experimental procedure is commonly done with 10 mg of solute per 1 mL of solvent at room temperature.[24,25] After this procedure you can blend two different solvents with different solubility parameters. As the ratio of solvents changes you can analyze which solvents the compound is most soluble in. These blended solvents can provide additional accuracy for the edge of the HSP sphere that individual solvents cannot provide. After completing this process multiple times with different solvents, you can refine the edge of your HSP sphere to better represent the solubility of your compound. HSP can be used computationally before experimentation to gain a general understanding of the HSP for a synthetic target. HSP can also be used after synthesis to selectively test green solvents that HSP says would work.

Based on some of the limitations found in many conjugated polymers, we want to design and incorporate side chains with a longer alkyl section which is capped with ionic or polar head functionalization, as shown in **Figure 4**. By adding a long insulating alkyl section between the polar group and the core of the polymer, we predict the detrimental changes in energy level found previously will be avoided in our materials. By maintaining the use of polar/ionic terminal side chains we also predict a shift in the HSP values of PTQ-10.

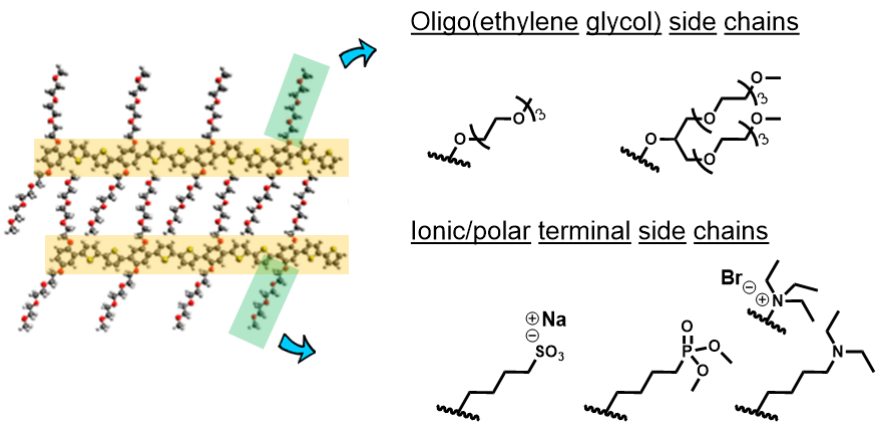


**Figure 4**. The top row shows side chains used in previous literature and the bottom row shows side chains we want to try.

HSP provides two mechanisms to increase green solvent processability. The first is to synthesize PTQ-10, measure solubility to find the HSP sphere, and then search literature for green solvents that fall within the HSP sphere. Solvents that are found to be green, and within PTQ-10's HSP sphere can then be selectively purchased and experimentally tested. The second is to undergo modifications to the PTQ-10 side chain. Synthesizing a new derivative with a polar/ionic group at the end of an alkyl section would change its solubility, thus its HSP sphere. Once the derivative is made, solubility and photovoltaic parameters will be found to measure the change caused by the new side chain.

# Experimental

All chemicals were purchased from commercial sources (Sigma-Aldrich, Fisher, Acros, etc.) and were used as received except when specified. For reactions under argon, the reaction flask was evacuated via vacuum and refilled with argon three times. All NMR analyses were run with a Bruker Ascend™ 400. All microwave reactions were run with a CEM discover system microwave reactor.

## Synthesis of 1,4-dibromo-2,3-difluoro-5,6-dinitrobenzene (**1**)

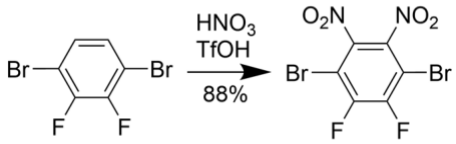


**Caution!** *Triflic acid is highly corrosive, reactive, and can cause burns or damage on contact. It was handled with proper PPE and reactants were added slowly to ensure a controlled reaction.*
**Caution!** *Nitric acid is highly corrosive, reactive, and can cause burns or damage on contact. It was handled with proper PPE and reactants were added slowly to ensure a controlled reaction.*

Fuming triflic acid (TfOH) (60 mL, 660 mmol, 34 eq) and a stir bar were added to a 250 mL round bottom flask (RBF) in an ice bath. Then nitric acid (4 mL, 31.8 mmol, 3.2 eq) was added slowly to ensure there was not an aggressive response from the reaction. Then the reaction was allowed to stir for one hour. After an hour, 1,4-dibromo-2,3-difluorobenzene (**0**) (5.45 g, 20.05 mmol, 1 eq) was

added in portions over the course of 20 minutes. Then the reaction was left to stir again for one hour. After the hour, nitric acid (4 mL, 31.8 mmol, 3.2 eq) was added to the reaction and then the reaction was allowed to stir for two hours at room temperature. After two hours, the reaction was heated for 18 hours at 70℃. The reaction was then allowed to cool to room temperature before being added to ice water (250 mL). It was then stirred for 15 minutes in the ice water and then collected with vacuum filtration. The collected product was dried over night on high vacuum. The product collected was a yellow powder. Yield: 6.380 g, 87.9%. $^{19}$F NMR (400 MHz, $CDCl_3$): $\delta$= -113.85. $^{13}$C NMR: $\delta$= 105.75, 105.99, 148.85, 151.31. Full spectra shown in Figures S1 and S2.

## Synthesis of 3,6-dibromo-4,5-difluoro-1,2-benzenediamine (**2**)

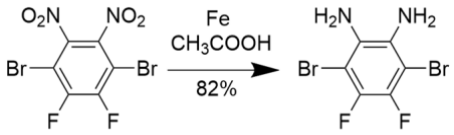


1,4-dibromo-2,3-difluoro-5,6-dinitrobenzene (**1**) (3.377 g, 8.29 mmol, 1 eq) was added with Fe powder (7.3 g, 116.25 mmol, 14 eq) in a 250 mL RBF and put under argon. After this, glacial acetic acid (100 mL, 1.73 mol, 209 eq) was added to the reaction, and the reaction was heated for 18 hours at 45℃. The reaction then was cooled to room temperature. While the reaction was cooling, 10% sodium hydroxide (200 mL) was cooled in an ice bath. Once the reaction cooled to room temperature it was added to the ice cold 10% sodium hydroxide. After that the reaction was filtered and dissolved in ethyl acetate. The ethyl acetate solution was washed with sodium bicarbonate solution four times. The organic layer was then dried with magnesium sulfate and the solution was filtered. Once filtered the solvent was evaporated using a rotovap and then dried overnight on high vacuum. The product collected was a white solid. Yield: 2.272 g, 81.8%. $^{1}$H NMR (400 MHz, $CDCl_3$): $\delta$= 3.83 (s, 4H). $^{13}$C NMR: $\delta$= 98.21, 98.31, 98.34, 98.43, 140.60, 140.78, 143.00, 143.18. $^{19}$F NMR: $\delta$= -139.06. Full spectra shown in Figures S3, S4, and S5.

## Synthesis of 5,8-dibromo-6,7-difluoroquinoxaline-2-ol (**3**)

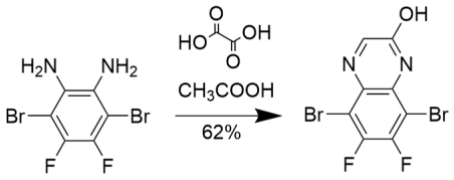


3,6-dibromo-4,5-difluorobenzene-1,2-diamine (**2**) (4.6 g, 15.5 mmol, 1 eq) and glyoxylic acid (1.1 g, 15.24 mmol, 1 eq) were added to a 250 mL RBF. The RBF was put under argon and then glacial acetic acid (120 mL, 2.08 mol, 277 eq) was added. The reaction was then heated to reflux for three hours and was allowed to cool. Then once cooled, it was extracted with dichloromethane and washed with water. The product was dried with magnesium sulfate and then the dichloromethane was removed with a rotovap. After this the product was recrystallized in ethanol and dried on high vacuum overnight. The product collected was a light beige solid. Yield: 1.571 g, 61.5%. $^{1}$H NMR (400 MHz, DMSO): $\delta$= 12.76 (s, 1H), 8.44 (s, 1H). $^{19}$F NMR (400 MHz, $CDCl_3$): $\delta$= -119.26, -119.32, -128.38, -128.44. Full spectra shown in Figures S6 and S7.

## Synthesis of 5,8-dibromo-6,7-difluoro-2-((2-hexyldecyl)oxy) Quinoxaline (**4**)

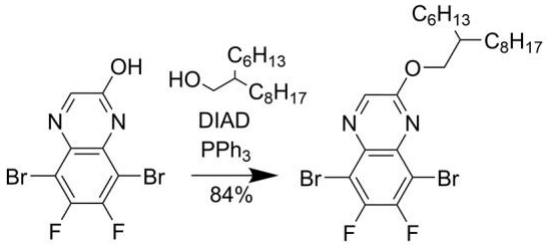


**Caution!** *DIAD is a health and environmental hazard. Proper PPE was used when handling and it was disposed of correctly*.

5,8-dibromo-6,7-difluoroquinoxalin-2-ol (**3**) (1.002 g, 0.61 mmol, 1 eq) and triphenylphosphine (0.857 g, 0.68 mmol, 1.11 eq) to a 200 mL RBF under argon. of anhydrous tetrahydrofuran (THF) (200 mL) was added to the RBF, and then the reaction was cooled in an ice bath. Once the reaction cooled to 0 ℃, 2-hexyldecan-1-ol (0.848 g, 0.65 mmol, 1.06 eq) was added to the RBF, and then DIAD (0.899 g, 0.915 mmol, 1.5 eq) was added slowly. Once the reactants were added the reaction was heated to reflux for 18 hours. Once the 18 hours were up the reaction was allowed to cool. Once cooled, distilled water was added and the mixture was extracted with dichloromethane. The organic layer was washed with water and then dried with magnesium sulfate. The organic layer was then filtered and the filtrate was concentrated. Once the filtrate was concentrated the triphenylphosphine oxide was precipitated out by adding dropwise to a large volume of hexanes. Then the product was purified by using column chromatography using a 12:1 hexanes/ethyl acetate mixture. The product collected was a white solid. Yield 1.396 g, 84%. $^1$H NMR (400 MHz, $CDCl_3$): $\delta$= 8.51 (s, 1H), 4.49 (d, $J$=5.65 Hz, 2H), 1.89 (p, $J$=5.87 Hz, 1H), 1.25-1.47 (m, 24H), 0.88 (td, $J$=6.90,2.51 Hz, 6H). Full spectra shown in Figure S8.

## Purification of $Pd_2(dba)_3 \cdot CHCl_3$

The catalyst ($Pd_2(dba)_3 \cdot CHCl_3$) was dissolved in the lowest amount of chloroform possible (>5 mL) in a 100 mL RBF. Acetone (20 mL) was also added to the RBF and then placed in a freezer overnight covered with aluminum foil. The next day the solid was collected with filtration and washed with cold acetone from the freezer. Solid was then placed under high vacuum to dry. This process was repeated until NMR characterization showed acceptable purification (88.9% pure) The following peaks listed are the ones used to calculate purity. The first peak represents free dba (impurity) and the other two represent the cis and trans conformations of $Pd_2(dba)_3 \cdot CHCl_3$. $^1$H NMR (400 MHz, $CDCl_3$): $\delta$= 7.63 (d, 0.30), 5.65 (d, 0.20), 5.33 (d, 1.00). To calculate the percentage of catalyst with dba, the integrations of each peak were used in a percentage calculation with the following formula. Full spectra shown in Figure S9.

$$\frac{\text{Major Isomer + Minor Isomer}}{\text{Major Isomer + Minor Isomer + }\left(\frac{\text{Free dba}}{2}\right)}$$

## Polymerization of PTQ-10 (**5**)

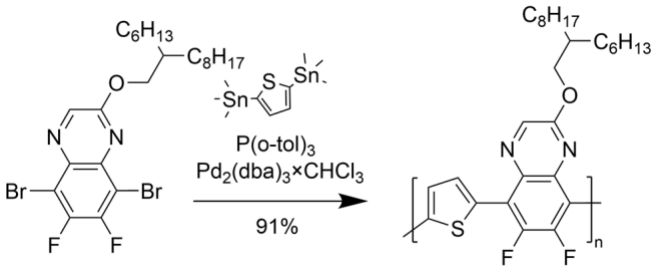


**Caution!** *Trimethyl tin bromide is a health hazard. Proper PPE was used when handling and it was disposed of carefully.*

5,8-dibromo-6,7-difluoro-2-((2-hexyldecyl)oxy) quinoxaline (**4**) (79.6 mg, 0.126 mmol, 1 eq), 2,5-bis(trimethylstannyl)thiophene (57.4 mg, 0.126 mmol, 1 eq), $Pd_2(dba)_3{\cdot}CHCl_3$ (2.9 mg, 0.0025 mmol, 0.02 eq), and P(*o*-tol)$_3$ (6.8 mg, 0.02 mmol, 0.16 eq) were added to a 10 mL microwave reactor vial. The vial was then put under argon, and anhydrous toluene (0.9 mL) was added under an argon stream. The reaction was then heated up to 200℃ in a CEM microwave reactor set to 300 W for 10 minutes. After polymerization, the crude polymer was dissolved in hot chlorobenzene and precipitated out in stirring room temperature methanol. The solvent was then collected and extracted with a Soxhlet extractor. The solvent systems used in the extraction were ethyl acetate, hexanes, and chloroform in order. The polymer was then collected in chloroform and concentrated down. The concentrated solution was then precipitated out with room temperature stirring chloroform. The precipitate was collected via filtration, and the product was dried over high vacuum overnight. The product collected was a purple solid**.**

**Table 1**: *Attempts with twice the amount of reactants used

| Attempt | Yield (%) |
|---|---|
| 1 | 62.3 mg (90.5%) |
| 2* | 115.7 mg (84.9%) |
| 3* | 106.1 mg (74.1%) |
| 4* | 78.1 mg (63.3%) |
| 5* | 77.0 mg (55.1%) |

## Solubility Testing

Twenty-two samples of 10 mg were measured out into 2 mL vials. Then these samples were introduced to 1 mL of a selected solvent and shaken. The solvents used were 2-propanol (IPA), methanol (MeOH), dichloromethane (DCM), acetone, ethanol (EtOH), ethyl acetate (EtoAc), chloroform ($CHCl_3$), cyclohexane, chlorobenzene (CB), ortho-xylene (oX), toluene, 1,4-dioxane, 1,8-cineole, limonene, 3-methylcyclohexanone, cyrene, tetrahydrofuran (THF), p-cymene, diethyl ether (DEE), cyclopentyl methyl ether (CPME), and water. Samples that showed partial solubility were heated to confirm status of soluble or insoluble. The status was then uploaded to a spreadsheet where the approximate Hansen Solubility Parameter values were calculated. This spreadsheet took

the values of solvents it was soluble and insoluble in to find the HSP point of PTQ-10. It also calculated the radius of the sphere around it to represent the solubility.
HSP_Calculations_PTQ10.xlsx

## Synthesis of 1-((6-bromohexyl)oxy)-4-methylbenzene (**8**)

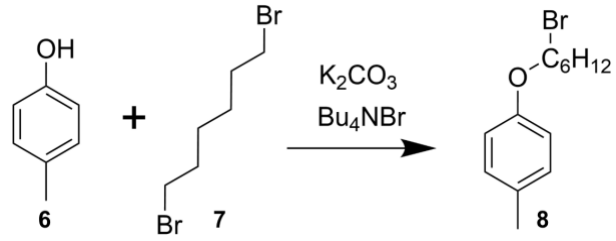


(0.779g, 7.20 mmol, 1 eq) of *p*-Cresol (**6**), (2.26g, 16.2 mmol, 2.25 eq) of potassium carbonate, (0.142g, 0.440 mmol, 0.061 eq) of $Bu_4NBr$, and a stir bar were added to a three necked RBF. The RBF was attached to a condensing column and put under argon. Once under argon (2.8 mL, 18.2 mmol, 2.5 eq) of 1,6-dibromohexane (**7**) and (70 mL) of acetone were syringed into the RBF. The reaction was then heated to 60°C for 48 hours. Once the reaction cooled down it was vacuum filtered, and the liquid was rotovaped down. Once rotovaped down the yellow oil was separated from the clear liquid and vacuum distilled. The vacuum distillation was run at 80°C and a yellow liquid was collected. Product was determined to be impure, so column chromatography was run in 6:1 Hex:EtOAc. Yield 1.34 g, 70%. $^1$H NMR (400 MHz, $CDCl_3$): δ (p.p.m.) 7.07 (d, 2H), 6.79 (d, 2H), 3.92 (t, 2H), 3.42 (t, 2H), 2.28 (s, 3H-1.83 (m, 2H), 1.83-1.73 (m, 2H), 1.55-1.44(m, 4H). Full spectra shown in Figure S10.

## Synthesis of 5,8-dibromo-6,7-difluoro-2-((6-(p-tolyloxy)hexyl)oxy) quinoxaline (**9**)

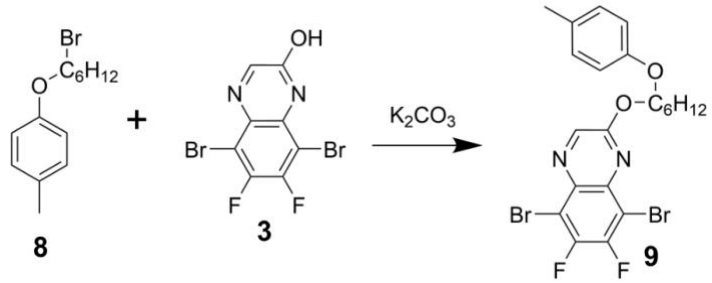


(0.498g, 1.47 mmol, 1.0 eq) of 5,8-dibromo-6,7-difluoroquinoxalin-2-ol (**3**), (448 mg, 1.68 mmol, 1.1 eq) of 1-[(6-Bromohexyl)oxy]-4-methylbenzene (**8**), and (198 mg, 1.76 mmol, 1.2 eq) of potassium t-butoxide were added to a 2 necked 100 mL RBF and dissolved in (30 mL) of methanol. The reaction was put at reflux for 12 hours and then cooled to room temperature. After cooling the reaction was mixed with saturated $NH_4Cl$, and then product was extracted with DCM. The extraction was washed with water and then dried with magnesium sulfate. After gravity filtration the liquid was rotovaped down to a yellow solid. A column was then run to purify the product at 5:1 Hex: EtOAc. After column chromatography, none of the fractions were found to have desired products. Yield 0 g, 0%. Full spectra of compound before column chromatography shown in figure S11.

## Synthesis of 5,8-dibromo-2-((6-bromohexyl)oxy)-6,7-difluoro quinoxaline (**10**)

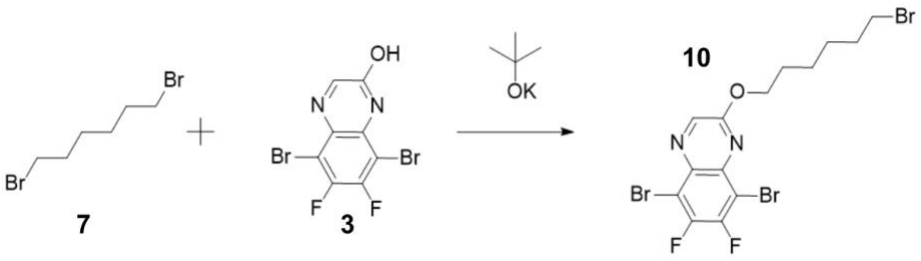


(170 mg, 0.5 mmol, 1.0 eq) of 5,8-dibromo-6,7-difluoroquinoxalin-2-ol (**3**), (198 mg, 1.76 mmol, 1.2 eq) of $(CH_3)_3COK$ and (308 mg, 1.26 mmol, 2.6 eq) of 1,6-dibromohexane (**7**) were added to a 100 mL RBF and dissolved in (25 mL) of methanol. The reaction was heated to reflux for 18 hours and then cooled to room temperature. After a TLC plate was taken, the reaction was confirmed to be incomplete. (123 mg, 0.451mmol, 0.9 eq) 1,6-dibromohexane was added to the reaction, and heat was applied for another 10 hours. After cooling, the reaction was mixed with saturated $NH_4Cl$, and then product was extracted with DCM. The extraction was washed with water and then dried with magnesium sulfate. After gravity filtration the liquid was rotovaped down to a yellow solid. A column was then run to purify the product at 4:1 Hex: EtOAc. After column chromatography, none of the fractions were found to have desired products.

## Synthesis of 5,8-dibromo-2-((6-bromohexyl)oxy)-6,7-difluoro quinoxaline (**10**)

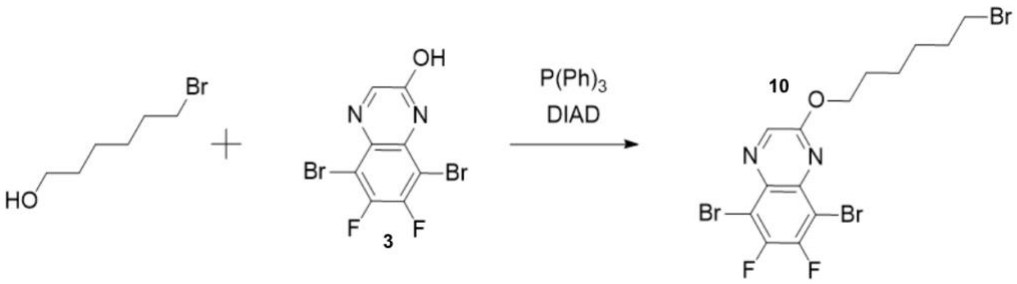


**Caution!** *DIAD is a health and environmental hazard. Proper PPE was used when handling and it was disposed of correctly.*

(207.4 mg, 0.6 mmol, 1.0 eq) of 5,8-dibromo-6,7-difluoroquinoxalin-2-ol (**3**) and (141.8 mg, 0.54 mmol, 0.9 eq) of $PPh_3$ were added to a 50 mL 2 necked RBF. The RBF was put under inert conditions, and then 20 mL of anhydrous THF were added to the flask. Then the RBF cooled in an ice bath as (104.6 mg, 0.57 mmol, 0.95 eq) of 6-bromohexanol and (182.3 mg, 0.90 mmol, 1.5 eq) of DIAD were slowly added to the solution. Then the reaction was heated to reflux for 18 hours and then cooled to room temperature. Water was then added to the reaction and extracted with DCM. The DCM was then washed with water and dried with magnesium sulfate. A column was then run to purify the product at 1:1 Hex: EtOAc.

# Results

## Synthesis of PTQ-10

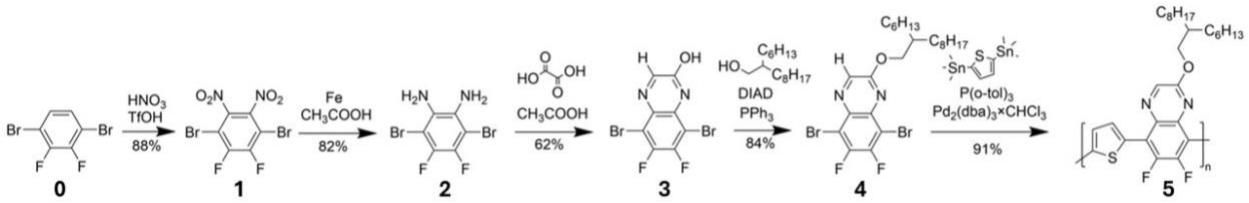


**Scheme 1**. Synthetic scheme of PTQ-10

To form PTQ-10 we began with an electrophilic aromatic substitution of **0** to form **1**, then a reduction reaction of **1** to make **2**. After synthesizing **2**, a condensation reaction was used to make **3**, and then a Mitsunobu was used to make **4**. The last step was a Stille cross coupling of **4** to make our finished polymer **5**. The electrophilic aromatic substitution to form **1** gave us a slightly higher yield than what was done in literature, with 88% compared to 85%.[22] The second reaction saw the largest decrease in yield compared to literature as it went from 94% to 82%. This was caused by the liquid separation. This process caused a high amount of emulsion, and even with brine the emulsion was difficult to work with. It was found that **2** was prone to degradation at room temperature so it was important to start the condensation reaction within a few days. The condensation reaction took multiple attempts to work when using the procedure from literature. Once we used glacial acetic acid without anhydrous ethanol the reaction was able to move forward. The Mitsunobu reaction to form **4** was a notable decrease in yield, with our reaction having an 84% yield compared to the 93% in literature. This completed the formation of our monomer, which was then used in a Stille cross coupling to make **5**. The Stille cross coupling was completed 5 times to synthesize the 250 mg necessary for solubility testing. As seen in **Table 1** the initial reactions resulted in high yields, however as the reaction was undergone multiple times the yield began decreasing. The yields began at 91%, which was slightly lower than the 97% in literature, but our last attempt had a yield of 55%. This was due to our catalyst degrading as it was exposed to air for each polymerization. Our polymerized material came out of the microwave reactor and formed a purple gel. The polymer was crashed out in methanol in which you could see individual strands begin to form. After the vacuum filtration at the end of the purification the polymer began forming strands that would intertwine for our higher molecular weight material. These strands would even begin turning gold as they dried on the vacuum filtration.

# PTQ-10 Solubility Testing

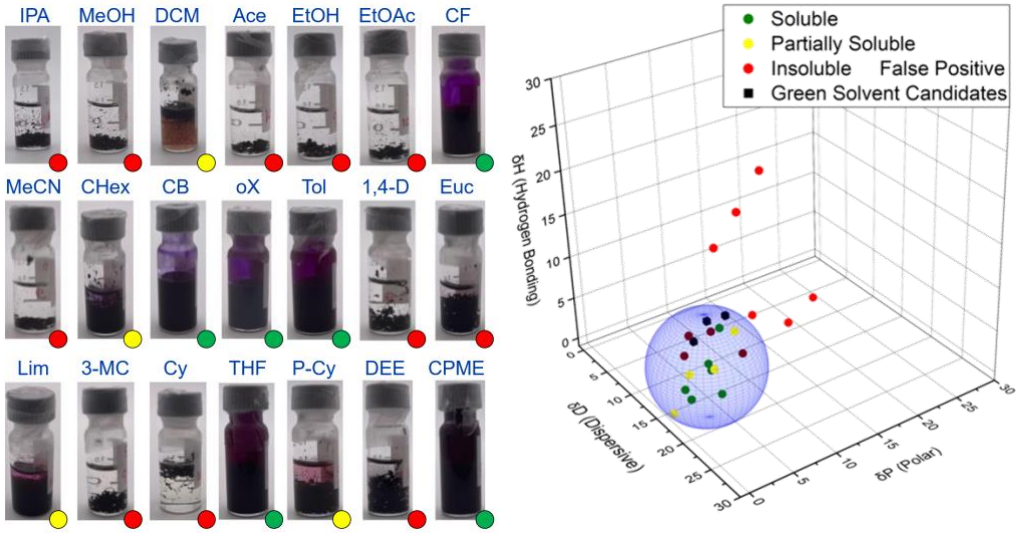


**Figure 5**. The left figure shows all the 1mL vials containing different solvents with PTQ-10. The right figure shows the HSP sphere created with the data collected from the solubility testing.

Once the material was made, we next focused on the characterization of solubility. **Figure 5** shows the result of attempting to dissolve PTQ-10 in a selection of different solvents. In the solubility testing of PTQ-10, the HSP sphere, shown in **Figure 5**, obtained from the solvents tested resulted in a sphere with similar placement to previous literature. However, the size of the sphere is slightly larger than the one from literature. This could be from several factors including that our solubility testing used less solvents, lower molecular weight material, and lacked the use of blended solvents. All the solvents outside of the sphere were insoluble. The solvents that showed as insoluble inside the sphere appeared in the space between our sphere and the sphere from previous work. With our material being a lower molecular weight and sphere showing larger we assume that the radius of our sphere calculated is an overestimation. To obtain more accurate spheres in future experiments, more solvents should be used with higher molecular weight material to ensure that low molecular weight material is not causing the polymer to dissolve easier.

a)

| Solvent | Waste | Enviro | H Health | Safety | Total | δD | δP | δH |
|---|---|---|---|---|---|---|---|---|
| Water | 4 | 9 | 9.5 | 9 | 7.4 | 15.5 | 16 | 42.3 |
| Lactic Acid | 6 | 7.5 | 6.5 | 9 | 7.2 | 17 | 8.3 | 28.4 |
| Propionic Acid | 5.5 | 6.5 | 7 | 7.5 | 6.6 | 14.7 | 5.3 | 12.4 |
| Methanesulfonic Acid | 5.5 | 6 | 7 | 7.5 | 6.5 | | | |
| Formic Acid | 5.75 | 8 | 4 | 7 | 6.0 | 14.6 | 10 | 14 |
| Acetic Acid (glacial) | 4.75 | 6 | 6 | 7 | 5.9 | 14.5 | 8 | 13.5 |
| 1,3-Propanediol | 6 | 8 | 9.5 | 10 | 8.2 | 16.8 | 13.5 | 23.2 |
| 1-Pentanol | 8 | 6.5 | 9.5 | 9.5 | 8.3 | 15.9 | 5.9 | 13.9 |
| 2-Ethyl hexanol | 8.75 | 6 | 8.5 | 9 | 8.0 | 15.9 | 3.3 | 11.8 |
| 1-Heptanol | 9 | 6 | 8.5 | 9.5 | 8.1 | 16 | 5.3 | 11.7 |
| Ethylene glycol | 6 | 9 | 8.5 | 10 | 8.2 | 17 | 11 | 26 |
| Di(ethylene glycol) | 6 | 9 | 8.5 | 9.5 | 8.1 | 16.6 | 12 | 19 |
| Tri(ethylene glycol) | 6 | 7.5 | 10 | 9.5 | 8.1 | 16 | 12.5 | 18.6 |
| 1,2-Propanediol | 6 | 8 | 8.5 | 10 | 8.0 | 16.8 | 10.4 | 21.3 |
| Benzyl alcohol | 7.25 | 7 | 8 | 9 | 7.8 | 18.4 | 6.3 | 13.7 |
| Isoamyl alcohol | 7.25 | 6 | 9.5 | 9 | 7.8 | 15.8 | 5.2 | 13.3 |
| 1-Octanol | 8.5 | 4.5 | 8.5 | 9.5 | 7.5 | 16 | 5 | 11.2 |
| Glycerol | 6 | 9 | 7 | 10 | 7.8 | 17.4 | 11.3 | 27.2 |
| 1,4-Butanediol | 5.5 | 8 | 8 | 10 | 7.7 | 16.6 | 11 | 20.9 |
| Cyclohexanol | 7.25 | 6.5 | 8 | 9 | 7.6 | 17.4 | 4.1 | 13.5 |
| Isobutanol | 5.25 | 8 | 7 | 8.5 | 7.1 | 15.1 | 5.7 | 15.9 |
| 2-Pentanol | 7 | 6.5 | 7 | 8.5 | 7.2 | 15.6 | 6.4 | 13.3 |

b)

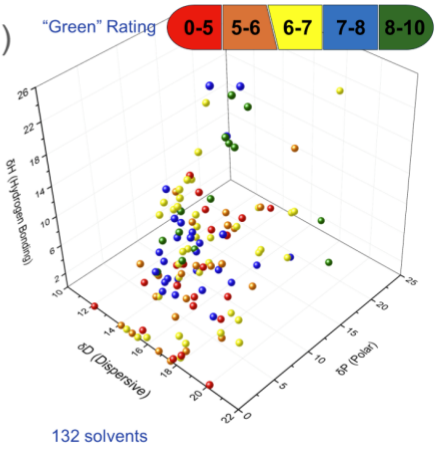


**Figure 6**. a) a snapshot of the data collected in the solvent database. b) HSP graph of 132 solvents from the solvent database with their greenness ratings.

In order to find a potential green solvent to dissolve PTQ-10, the HSP sphere can be overlaid on the 132 plotted solvents, which are shown in **Figure 6**. With focusing on the best potential candidates, there were three solvents that fulfilled the requirements of lying within PTQ-10's solubility sphere and obtaining a greenness rating over eight by GSK standards. These were glycerol triacetate, isobutyl acetate, and diethyl succinate. With new solvents computationally found, the computational system needs to be tested by purchasing these solvents and experimentally using them with PTQ-10.

## Synthesis of PTQ-10 Derivative

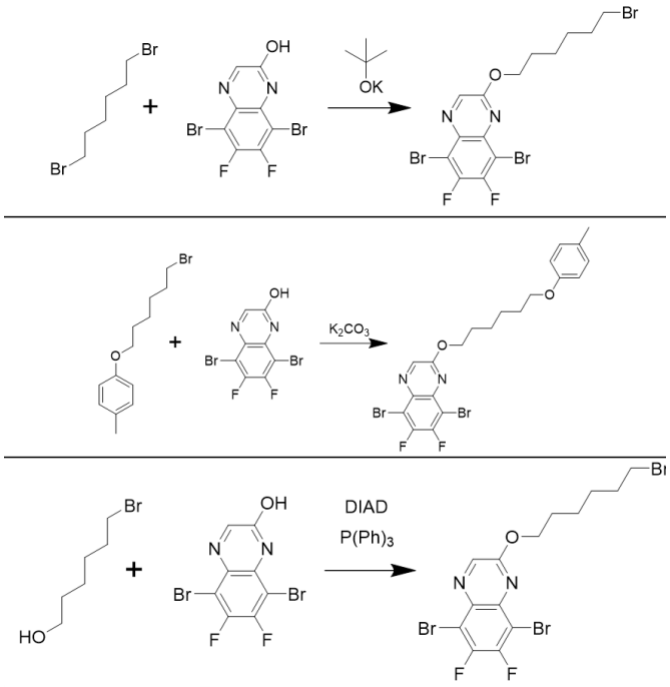


**Scheme 2**. Synthetic scheme of the varying reactions attempted to add the novel side chain to the quinoxaline core.

In the top synthesis of **Scheme 2**, an $S_N2$ reaction was attempted with tert-butoxide to add 1,6-dibromohexane to the quinoxaline core. This reaction was unable to go forward. We predicted that this was due to side reactions such as dimerization due to having two reactive bromines. To negate these side reactions, a protection group was added that was found from literature. The synthesis followed closely with what was found in literature, with only a minor decrease in yield from 75% to 70%.[28] After this protection reaction, a similar $S_N2$ reaction was attempted, with the only difference being potassium carbonate used as the base instead of tert-butoxide. The addition of the protected side chain also did not proceed efficiently. This reaction was attempted multiple times with tert-butoxide and potassium carbonate as bases with acetone and methanol used as solvents. None of these attempts were successful, and after column chromatography and NMR spectroscopy, it was found that the novel side chain and quinoxaline core simply were not reacting. This is due to the alcohol on quinoxaline being less acidic than initially anticipated or a more

dramatic change in the reactivity of the electrophile. To continue synthesis without an $S_N2$ reaction, we used the Mitsunobu reaction from PTQ-10 synthesis to add the novel side chain. The first attempt at this reaction formed a red product that was not our desired product. However, on the second attempt the temperature was raised 10°C and on this attempt, the desired product was found. Purification of this material was difficult however, as triphenylphosphine oxide is an abundant impurity found in Mitsunobu reactions. However, with this novel side chain being successfully added, modifications to add new polar or ionic groups to the end of an alkyl chain should be simpler. A simple amination of the end of the side chain would provide a simple polar group to test solubility and photovoltaic parameters.

# Conclusion

Addressing issues with the processability of organic solar cells is an important step to realizing their commercial applications. The unique attributes of lightweight, flexibility, and semi-transparency of OSCs can serve as a complimentary technology to current silicon solar panels. Reducing the reliance of fossil fuels should be of paramount importance.

This work made gains in the improvement of organic solar cell processability in two primary means. First, we demonstrated an approach to use HSP to help screen hundreds of solvents without having to use a guess-and-check approach for solubility. Through the successful modelling of the PTQ-10 solubility sphere, we identified a few unique solvents worth further exploration. The next steps include testing the solubility of PTQ-10 in the new solvents of glycerol triacetate, isobutyl acetate, and diethyl succinate. By testing these solvents experimentally, we can also measure the accuracy of our model and determine if this computational method is sufficient.

Second, we helped to troubleshoot the synthetic methodology of adding new side chains on the PTQ core structure. This work identified a more effective route to change the side chain without additional synthetic complexity. The next step for the second technique is to add polar/ionic groups to the end of the side chain to synthesize a new material. This material should then be tested for solubility and photovoltaic parameters and compared to PTQ-10.

# Acknowledgements

I want to thank the McCullough Fellowship for their generous support of finances as I work on this project through the summer and fall of 2025. I also want to thank Dr. Jeromy Rech for the opportunity to work on this research project under his mentorship and guidance. Finally, I would like to thank Rich Miller for his contributions to this project through synthesis towards the development of this research.

# References

(1) Counts, T. W. *Interesting Facts on Energy - Fun Facts About Energy Consumption*.

https://www.theworldcounts.com/challenges/climate-change/energy (accessed 2024-12-09).
(2) Burek, S. *When will Fossil Fuels Finally Run Out and What is the Technical Potential for Renewable Energy Resources? | EBSCOhost*. https://openurl.ebsco.com/contentitem/gcd:55830446?sid=ebsco:plink:crawler&id=ebsco:gcd:55830446 (accessed 2024-12-09).
(3) *All the advantages of solar energy*. https://www.enelgreenpower.com/learning-hub/renewable-energies/solar-energy/advantages-solar-energy (accessed 2024-12-09).
(4) Lee, Y.; Park, C.; Balaji, N.; Lee, Y.-J.; Dao, V. A. High-Efficiency Silicon Solar Cells: A Review. *Isr. J. Chem.* **2015**, *55* (10), 1050–1063. https://doi.org/10.1002/ijch.201400210.
(5) *How a Solar Cell Works*. American Chemical Society. https://www.acs.org/education/chemmatters/past-issues/archive-2013-2014/how-a-solar-cell-works.html (accessed 2024-12-09).
(6) *Solar Panels – How Solar Panels Work? – Physics and Radio-Electronics*. https://www.physics-and-radio-electronics.com/blog/solar-panels-solar-panels-work/ (accessed 2025-04-26).
(7) Kang, J.; Kim, S. Y.; Zong, K. Facile Synthesis of Dithienobenzothiadiazoles and D18−Cl Polymer via Na2S-Mediated Rapid Thiophene-Annulations for Organic Solar Cells. *ChemSusChem* **2024**, *17* (17), e202400055. https://doi.org/10.1002/cssc.202400055.
(8) Zhao, F.; Dai, S.; Wu, Y.; Zhang, Q.; Wang, J.; Jiang, L.; Ling, Q.; Wei, Z.; Ma, W.; You, W.; Wang, C.; Zhan, X. Single-Junction Binary-Blend Nonfullerene Polymer Solar Cells with 12.1% Efficiency. *Adv. Mater.* **2017**, *29* (18), 1700144. https://doi.org/10.1002/adma.201700144.
(9) Chen, L.; Yi, J.; Ma, R.; Dela Peña, T. A.; Luo, Y.; Wang, Y.; Wu, Y.; Zhang, Z.; Hu, H.; Li, M.; Wu, J.; Zhang, G.; Yan, H.; Li, G. 19% Efficiency in Organic Solar Cells of Benzo[1,2-b:4,5-B']Difuran-Based Donor Polymer Realized by Volatile + Non-Volatile Dual-Solid-Additive Strategy. *Mater. Sci. Eng. R Rep.* **2024**, *159*, 100794. https://doi.org/10.1016/j.mser.2024.100794.
(10) Wu, P.-T.; Bull, T.; Kim, F. S.; Luscombe, C. K.; Jenekhe, S. A. Organometallic Donor−Acceptor Conjugated Polymer Semiconductors: Tunable Optical, Electrochemical, Charge Transport, and Photovoltaic Properties. *Macromolecules* **2009**, *42* (3), 671–681. https://doi.org/10.1021/ma8016508.
(11) Wadsworth, A.; Moser, M.; Marks, A.; S. Little, M.; Gasparini, N.; J. Brabec, C.; Baran, D.; McCulloch, I. Critical Review of the Molecular Design Progress in Non-Fullerene Electron Acceptors towards Commercially Viable Organic Solar Cells. **2019**. https://doi.org/10.1039/C7CS00892A.
(12) *Flexible and Semitransparent Organic Solar Cells - Li - 2018 - Advanced Energy Materials - Wiley Online Library*. https://advanced.onlinelibrary.wiley.com/doi/full/10.1002/aenm.201701791 (accessed 2025-07-22).
(13) Polman, A.; Knight, M.; Garnett, E. C.; Ehrler, B.; Sinke, W. C. Photovoltaic Materials: Present Efficiencies and Future Challenges. *Science* **2016**, *352* (6283), aad4424. https://doi.org/10.1126/science.aad4424.
(14) Wang, D.; Liu, H.; Li, Y.; Zhou, G.; Zhan, L.; Zhu, H.; Lu, X.; Chen, H.; Li, C.-Z. High-Performance and Eco-Friendly Semitransparent Organic Solar Cells for Greenhouse Applications. *Joule* **2021**, *5* (4), 945–957. https://doi.org/10.1016/j.joule.2021.02.010.
(15) Ravishankar, E.; Charles, M.; Xiong, Y.; Henry, R.; Swift, J.; Rech, J.; Calero, J.; Cho, S.; Booth, R. E.; Kim, T.; Balzer, A. H.; Qin, Y.; Ho, C. H. Y.; So, F.; Stingelin, N.; Amassian, A.; Saravitz, C.; You, W.; Ade, H.; Sederoff, H.; O'Connor, B. T. Balancing Crop Production and Energy Harvesting in Organic Solar-Powered Greenhouses. *Cell Rep. Phys. Sci.* **2021**, *2* (3). https://doi.org/10.1016/j.xcrp.2021.100381.
(16) Kawano, K.; Pacios, R.; Poplavskyy, D.; Nelson, J.; Bradley, D. D. C.; Durrant, J. R. Degradation

of Organic Solar Cells Due to Air Exposure. *Sol. Energy Mater. Sol. Cells* **2006**, *90* (20), 3520–3530. https://doi.org/10.1016/j.solmat.2006.06.041.

(17) Hermenau, M.; Riede, M.; Leo, K.; Gevorgyan, S. A.; Krebs, F. C.; Norrman, K. Water and Oxygen Induced Degradation of Small Molecule Organic Solar Cells. *Sol. Energy Mater. Sol. Cells* **2011**, *95* (5), 1268–1277. https://doi.org/10.1016/j.solmat.2011.01.001.

(18) Alder, C. M.; Hayler, J. D.; Henderson, R. K.; Redman, A. M.; Shukla, L.; Shuster, L. E.; Sneddon, H. F. Updating and Further Expanding GSK's Solvent Sustainability Guide. *Green Chem.* **2016**, *18* (13), 3879–3890. https://doi.org/10.1039/C6GC00611F.

(19) Neu, J.; Samson, S.; Ding, K.; Rech, J. J.; Ade, H.; You, W. Oligo(Ethylene Glycol) Side Chain Architecture Enables Alcohol-Processable Conjugated Polymers for Organic Solar Cells. *Macromolecules* **2023**, *56* (5), 2092–2103. https://doi.org/10.1021/acs.macromol.2c02259.

(20) Kong, X.; Zhang, J.; Meng, L.; Sun, C.; Qin, S.; Zhu, C.; Zhang, J.; Li, J.; Wei, Z.; Li, Y. 18.55% Efficiency Polymer Solar Cells Based on a Small Molecule Acceptor with Alkylthienyl Outer Side Chains and a Low-Cost Polymer Donor PTQ10. *CCS Chem.* **2022**, *5* (4), 841–850. https://doi.org/10.31635/ccschem.022.202202056.

(21) Sun, C.; Pan, F.; Bin, H.; Zhang, J.; Xue, L.; Qiu, B.; Wei, Z.; Zhang, Z.-G.; Li, Y. A Low Cost and High Performance Polymer Donor Material for Polymer Solar Cells. *Nat. Commun.* **2018**, *9* (1), 743. https://doi.org/10.1038/s41467-018-03207-x.

(22) Rech, J. J.; Neu, J.; Qin, Y.; Samson, S.; Shanahan, J.; Josey III, R. F.; Ade, H.; You, W. Designing Simple Conjugated Polymers for Scalable and Efficient Organic Solar Cells. *ChemSusChem* **2021**, *14* (17), 3561–3568. https://doi.org/10.1002/cssc.202100910.

(23) Zhao, K.; Zhang, Q.; Chen, L.; Zhang, T.; Han, Y. Nucleation and Growth of P(NDI2OD-T2) Nanowires via Side Chain Ordering and Backbone Planarization. *Macromolecules* **2021**, *54* (5), 2143–2154. https://doi.org/10.1021/acs.macromol.0c02436.

(24) Burgués-Ceballos, I.; Machui, F.; Min, J.; Ameri, T.; Voigt, M. M.; Luponosov, Y. N.; Ponomarenko, S. A.; Lacharmoise, P. D.; Campoy-Quiles, M.; Brabec, C. J. Solubility Based Identification of Green Solvents for Small Molecule Organic Solar Cells. *Adv. Funct. Mater.* **2014**, *24* (10), 1449–1457. https://doi.org/10.1002/adfm.201301509.

(25) Jalan, I.; Lundin, L.; van Stam, J. Using Solubility Parameters to Model More Environmentally Friendly Solvent Blends for Organic Solar Cell Active Layers. *Materials* **2019**, *12* (23), 3889. https://doi.org/10.3390/ma12233889.

(26) Lee, S.; Jeong, D.; Kim, C.; Lee, C.; Kang, H.; Woo, H. Y.; Kim, B. J. Eco-Friendly Polymer Solar Cells: Advances in Green-Solvent Processing and Material Design. *ACS Nano* **2020**, *14* (11), 14493–14527. https://doi.org/10.1021/acsnano.0c07488.

(27) Chen, Z.; Yan, L.; Rech, J. J.; Hu, J.; Zhang, Q.; You, W. Green-Solvent-Processed Conjugated Polymers for Organic Solar Cells: The Impact of Oligoethylene Glycol Side Chains. *ACS Appl. Polym. Mater.* **2019**, *1* (4), 804–814. https://doi.org/10.1021/acsapm.9b00044.

(28) Duan, C.; Cai, W.; Hsu, B. B. Y.; Zhong, C.; Zhang, K.; Liu, C.; Hu, Z.; Huang, F.; Bazan, G. C.; Heeger, A. J.; Cao, Y. Toward Green Solvent Processable Photovoltaic Materials for Polymer Solar Cells: The Role of Highly Polar Pendant Groups in Charge Carrier Transport and Photovoltaic Behavior. *Energy Environ. Sci.* **2013**, *6* (10), 3022–3034. https://doi.org/10.1039/C3EE41838C.

(29) Sun, C.; Pan, F.; Bin, H.; Zhang, J.; Xue, L.; Qiu, B.; Wei, Z.; Zhang, Z.-G.; Li, Y. A Low Cost and High Performance Polymer Donor Material for Polymer Solar Cells. *Nat. Commun.* **2018**, *9* (1), 743. https://doi.org/10.1038/s41467-018-03207-x.

# Supporting Information

**Figure S1**

Synthesis of 1,4-dibromo-2,3-difluoro-5,6-dinitrobenzene

$^{19}$F NMR

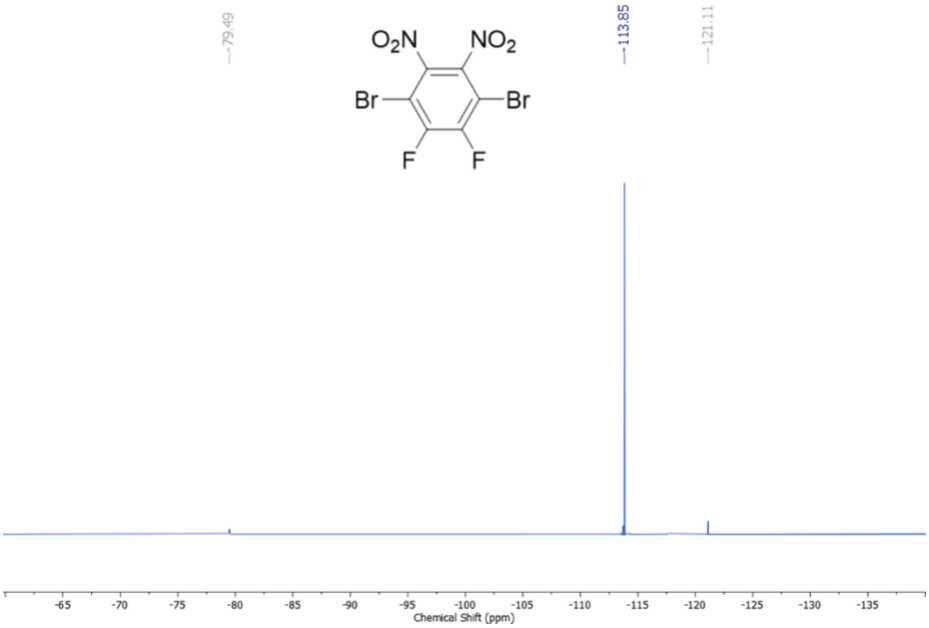


**Figure S2**

$^{13}$C NMR

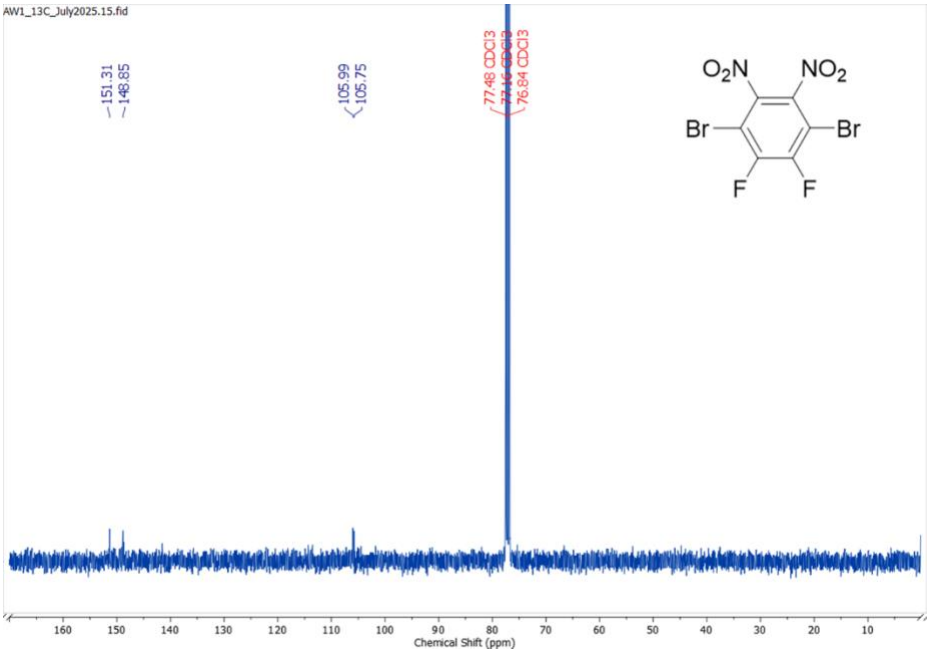

**Figure S3**

Synthesis of 3,6-dibromo-4,5-difluoro-1,2-benzenediamine

$^{1}$H NMR

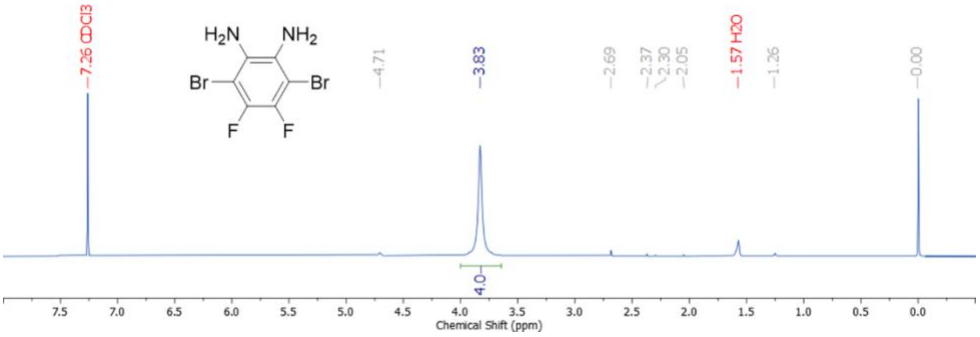


**Figure S4**

C$^{13}$ NMR

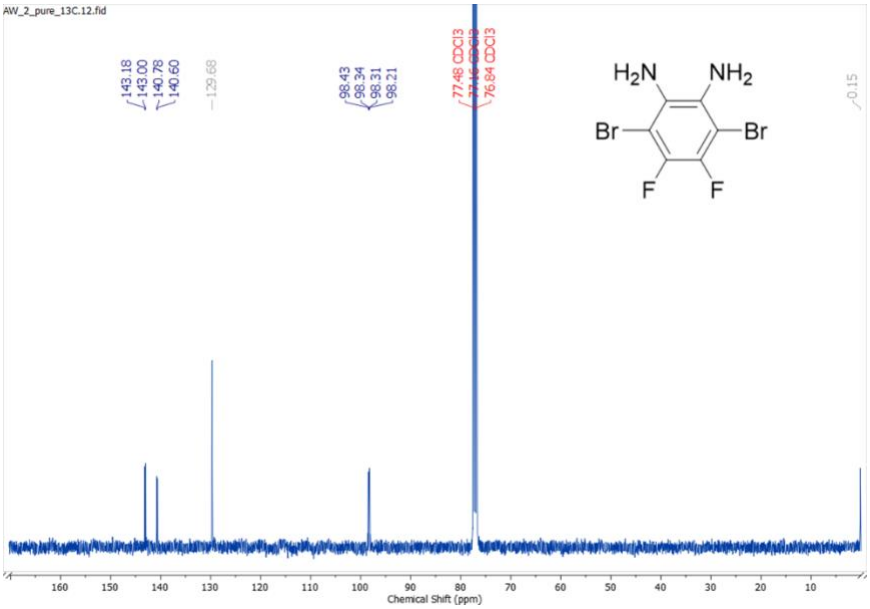


**Figure S5**

$^{19}$F NMR

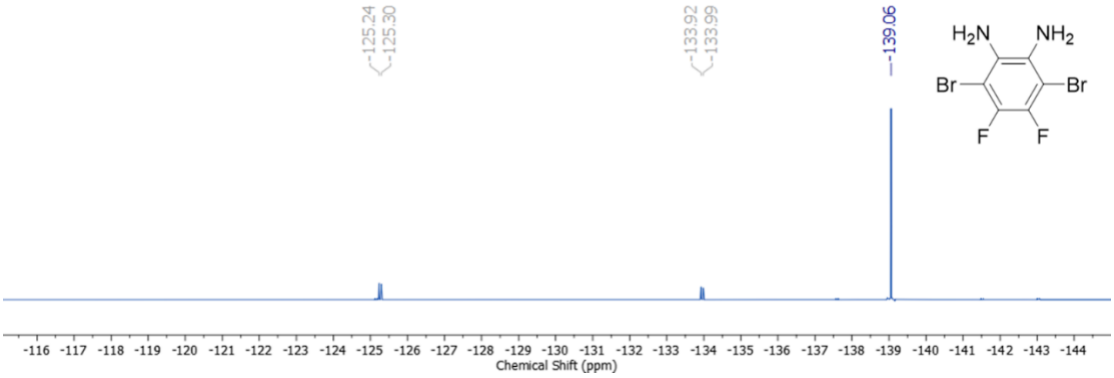

**Figure S6**

Synthesis of 5,8-dibromo-6,7-difluoroquinoxaline-2-ol

$^{1}$H NMR

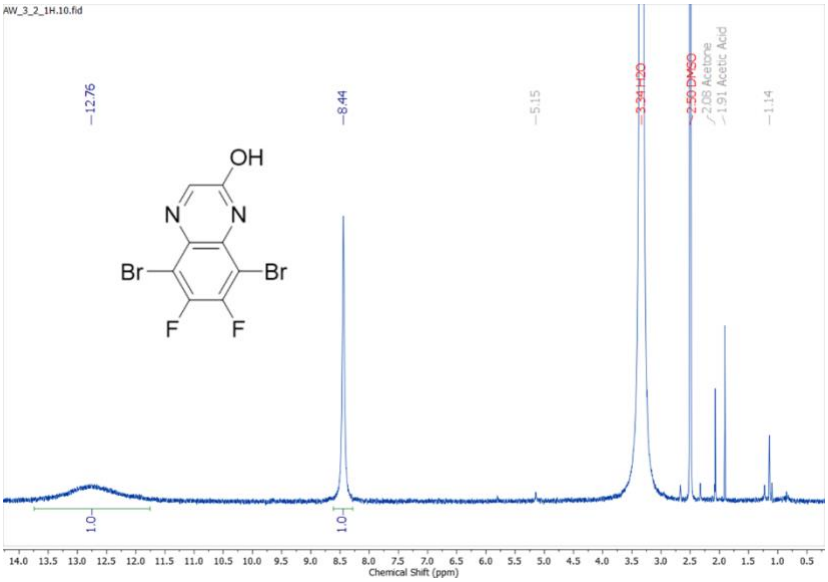


**Figure S7**

$^{19}$F NMR

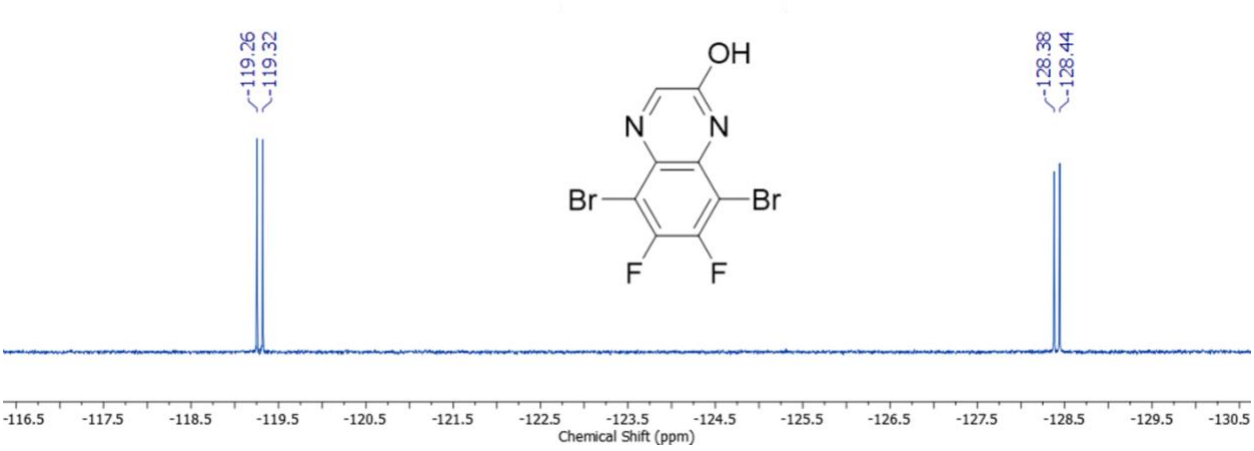

**Figure S8**

Synthesis of 5,8-dibromo-6,7-difluoro-2-((2-hexyldecyl)oxy) quinoxaline

$^{1}$H NMR

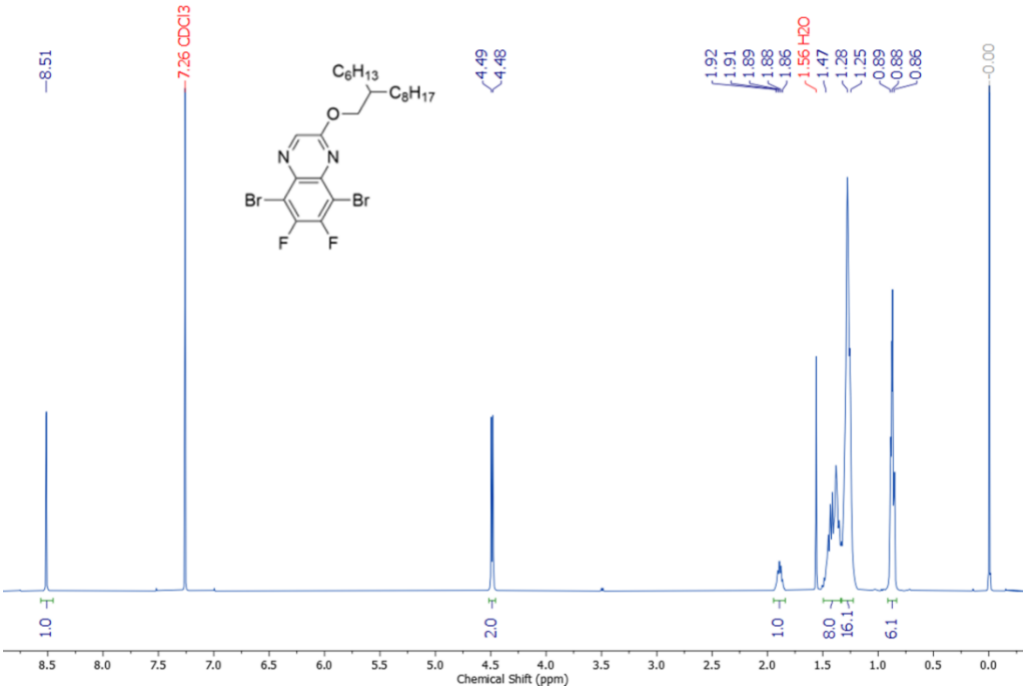

**Figure S9**

Purification of $Pd_2(dba)_3 \cdot CHCl_3$

$^1H$ NMR

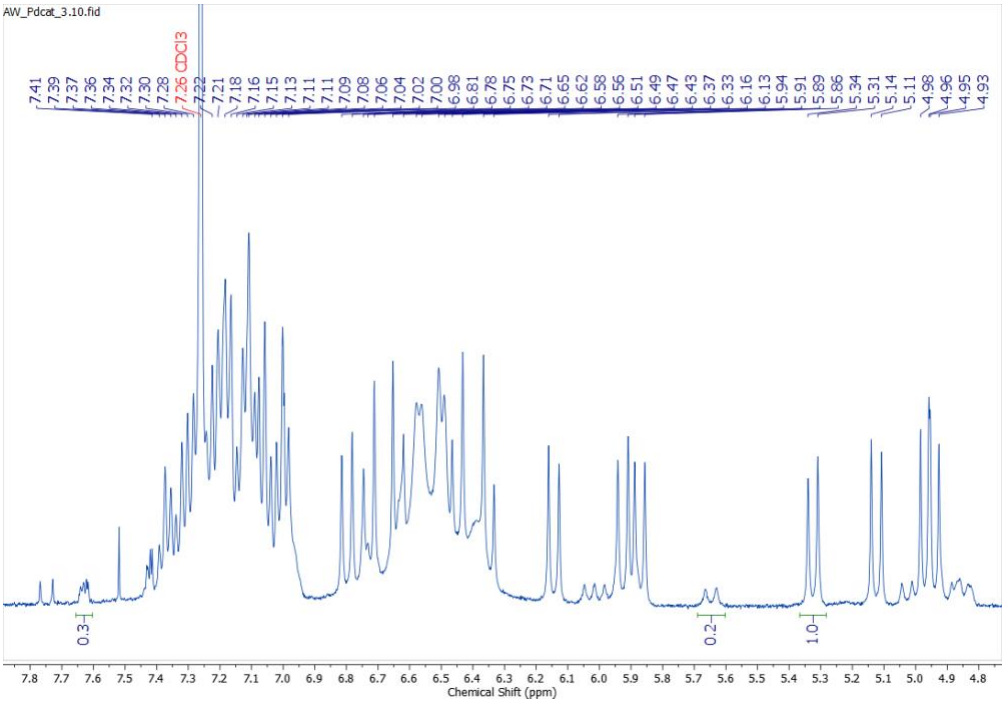


**Figure S10**

Synthesis of 1-((6-bromohexyl)oxy)-4-methylbenzene

$^1H$ NMR

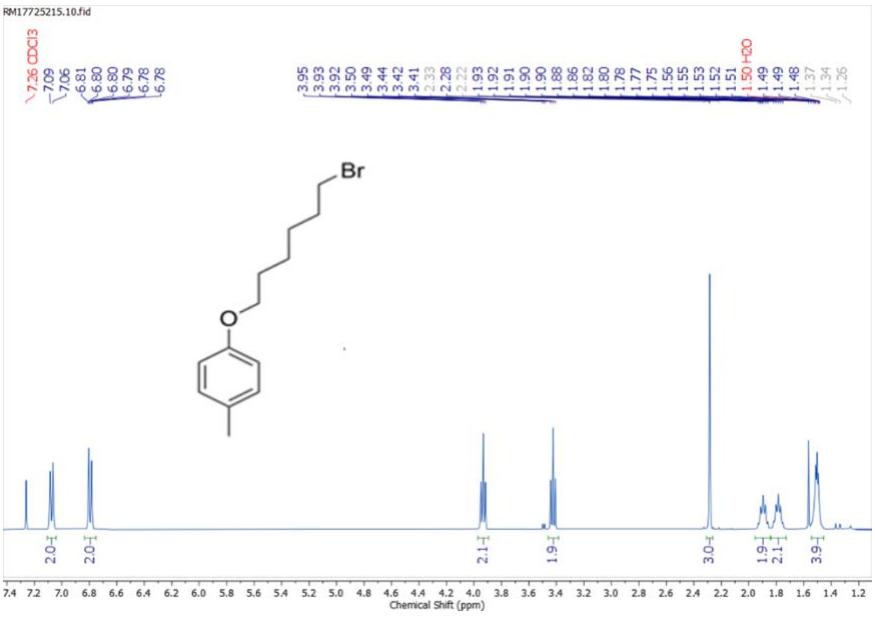

**Figure S11**

Synthesis of 5,8-dibromo-6,7-difluoro-2-((6-(p-tolyloxy)hexyl)oxy) quinoxaline

$^{1}$H NMR

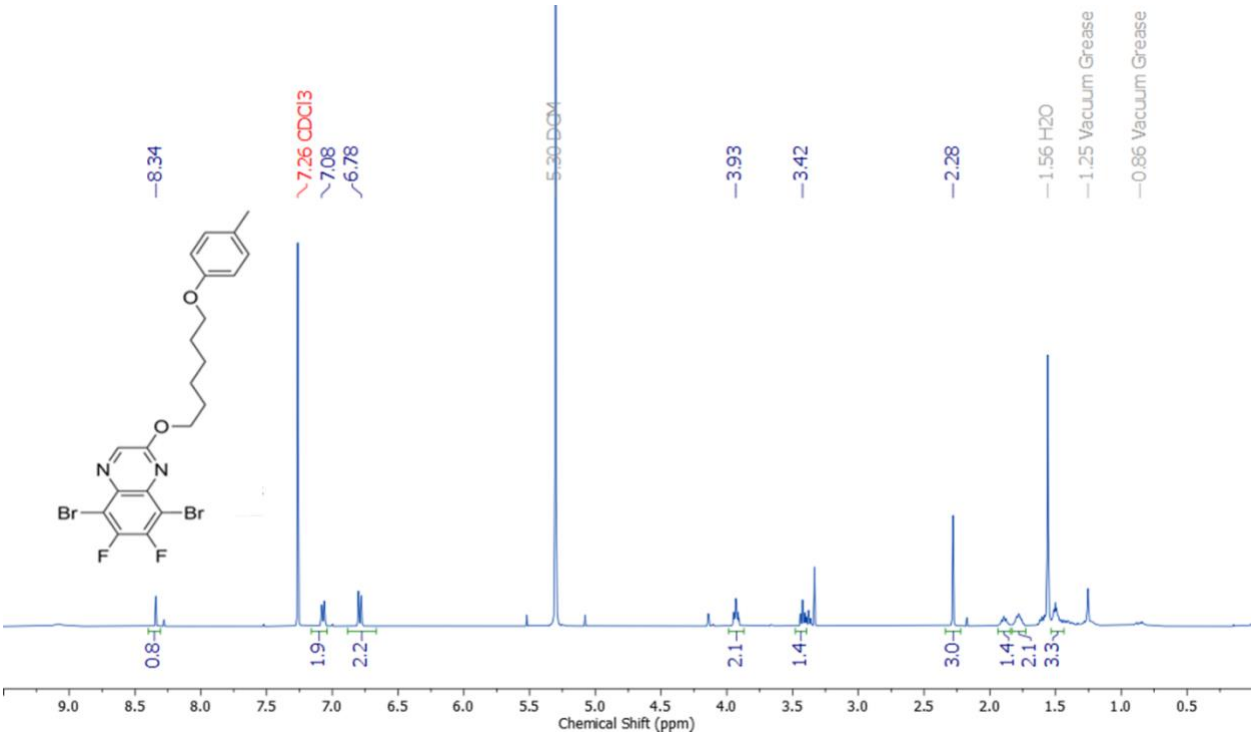

**Figure S12**

Synthesis of 5,8-dibromo-2-((6-bromohexyl)oxy)-6,7-difluoroquinoxaline

$^{19}$FNMR

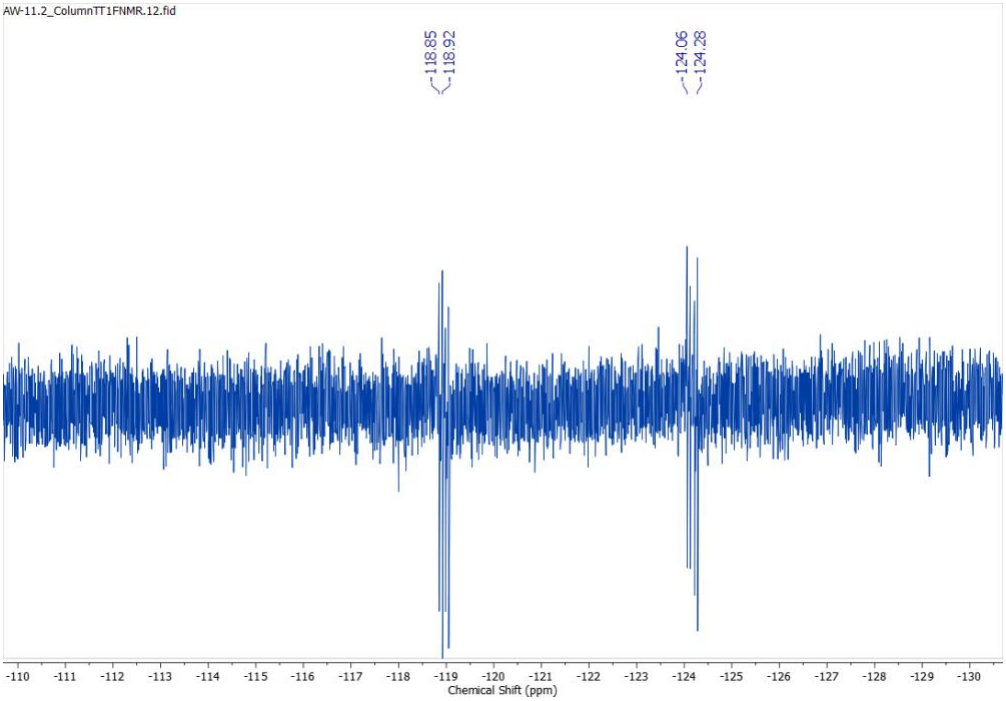


$^{1}$HNMR